Hindawi
Advances in Civil Engineering
Volume 2018, Article ID 2567438, 8 pages
https://doi.org/10.1155/2018/2567438

Research Article

Dynamic Fracture Toughness and Dynamic Tensile Strength of the Rock from Different Depths of Beijing Datai Well

Ke Man [1,2] **and Xiaoli Liu** [3]

[1] *Division of Environment Engineering, Beijing Research Institute of Uranium Geology, Beijing 100029, China*
[2] *Key Laboratory of China National Nuclear Corporation on High Level Radioactive Waste Geological Disposal, Beijing 100029, China*
[3] *State Key Laboratory of Hydroscience and Hydraulic Engineering, Tsinghua University, Beijing 100084, China*

Correspondence should be addressed to Ke Man; man_ke@sina.cn

Received 25 January 2018; Revised 5 June 2018; Accepted 27 June 2018; Published 29 August 2018

Academic Editor: Melina Bosco

From the standard test method suggested by ISRM and GB/T50266-2013, the uniaxial static tensile strength, dynamic tensile strength, and dynamic fracture toughness of the same basalt at different depths have been measured, respectively. It is observed that there may be an empirical relation between dynamic fracture toughness and dynamic tensile strength. The testing data show that both the dynamic fracture toughness and dynamic tensile strength increase with the loading rate and the dynamic tensile strength increases a little bit more quickly than the dynamic fracture toughness. With an increasing depth, the dynamic tensile strength has much more influence on the dynamic fracture toughness, as which it is much liable to bring out the unexpected catastrophes in the engineering projects, especially during the excavation at deep mining. From the rock failure mechanisms, it is pointed out that the essential reason of the rock failure is the microcrack unstable propagation. The crack processes growth, propagation, and coalescence are induced by tensile stress, not shear stress or compressive stress. The paper provides estimation of the dynamic fracture toughness from the dynamic tensile strength value, which can be measured more easily.

1. Introduction

Rock failure results from the propagation of one or more cracks and thus can be considered as a fracture mechanics problem [1–6]. The cracks processes growth, propagation, and coalescence and the LEFM (linear elastic fracture mechanics) can be widely used to describe the procession [7–10]. It follows that the fracture toughness of rock is important in theoretical studies and engineering applications related to rock failure. Three methods for measuring the fracture toughness have been suggested by ISRM so far [11, 12]. Though these testing methods are standard, application for describing rock mechanics properties is not widespread. As specimen preparation needs a long time [13], a simple and easy method for determining fracture toughness of rock would be helpful.

Whittaker et al. [14] obtained the relation between Mode I fracture toughness and the tensile strength, as follows:

$$\sigma_t = 9.35K_{IC} - 2.53, \tag{1}$$

where σ_t and K_{IC} are the tensile strength and Mode I fracture toughness of rock, respectively, with a coefficient of determination $r^2 = 0.62$. For $\sigma_t = 0$, K_{IC} is equal to 0.27. It means that rock with a zero tensile strength can resist crack propagation to a certain extent. However, as we know, it is impossible for any rock materials. As for $\sigma_t = 0$, K_{IC} should also be zero.

Zhang [15] has obtained another relation between Mode I fracture toughness and tensile strength by using a lot of experiment data. The relation can be expressed as

$$\sigma_t = 6.88K_{IC}, \tag{2}$$

where the coefficient of determination r^2 is 0.94. For this equation, when the σ_t is zero, K_{IC} is also zero.

Xie and Wang et al. [16, 17] have already tested the clay and obtained another equation between the fracture toughness and tensile strength:

$$K_{IC} = 0.3546\sigma_t, \quad (3)$$

where the coefficient of determination r^2 is 0.88.

Above references have shown that the Mode I fracture toughness has a relation with the tensile strength. However, the papers dealing with the dynamic fracture toughness and strength of rock have still been few so far. Therefore, this paper considers the relation between dynamic fracture toughness and dynamic tensile strength of the same basalt obtained from different depths and attempts to discuss the reason why the relation exists.

2. Measurement of Uniaxial Tensile Strength

2.1. Sampling and Rock Specimen Preparation. The tested rock is basalt, from the Nandaling group Mentougou area, derived from Datai well field VII, and the basalt explored from the heights +190 m, +90 m, and −10 m, respectively. Corresponding to the heights, the depths are 410 m, 510 m, and 610 m from the surface, respectively.

According to "Standard for test methods of engineering rock masses: GB/T50266-2013" [18], the tensile strength of the basalt can be measured by the Brazilian split method. And the specimen size is $\Phi 50\,\text{mm} \times H25\,\text{mm}$.

2.2. Testing Equipment and Measuring Principle. Brazilian split test was carried out by using the servo-controlled rock mechanics testing system RMTS150 in Sichuan University. The testing equipment is shown in Figure 1, and the parameters of the equipment are expressed in Table 1.

The Brazilian split test is a more general method for measuring rock tensile strength. It is an indirect method. Firstly, by forcing the disc at the two edges, ensure the stress of disc along the center line under uniform tensile stress condition. Secondly, obtain the tensile strength from the pressure corresponding to the failure point. And the calculation is as follows:

$$\sigma_t = \frac{2P}{\pi D t}, \quad (4)$$

where P is the maximum load during the Brazilian split test and D and t are the diameter and thickness of the rock specimen, respectively.

2.3. Testing Process. The specimens were manufactured under air-dry condition; meanwhile, the test was carried out at room temperature. The testing process is described as follows: firstly, through the disc edges of the diameter, scratch one pair loading parallel line on the disc edge surface. Secondly, modify the filler strip station of the testing system and place the specimen on the filler strip along the loading line. Thirdly, preforce the specimen several kN to fix the specimen and ensure the filler strip and specimen were kept in the same loading direction. Then, stop the preforcing until the specimen is fixed and steady, and close the bulletproof door.

The next step is the loading, which means that the force-control program is applied to with a loading rate of 5 kN/min. And the loading process stops when the specimen is totally cracked. Afterwards, the tensile strength can be obtained through the maximum pressure load, corresponding to the failure point during the press procession.

3. Measurement of Dynamic Tensile Strength

3.1. Sampling and Rock Specimen Preparation. The samples used in dynamic testing were cored from basalt blocks obtained from Datai well field VII. The cored diameter is 50 mm and the designed ratio of length to diameter ($L = D$) is 0.5. A number of samples were cut into two series for investigating the influence of dynamic tensile strength and dynamic fracture toughness on the rock. Especially, the same cores could be divided into two series of specimens: one is for the dynamic tensile strength measurement and the other is for the dynamic fracture toughness measurement. The surfaces of all the samples were then ground to achieve good contact on the surfaces with the pressure bars.

Prior to conducting the tests, all the test samples were labelled and weighed and their dimensions measured. The sequence of cutting the samples from each core was recorded.

3.2. Testing Equipment and Measuring Principle. The SHPB (Split Hopkinson pressure bar) is a common experimental technique nowadays for testing the dynamic performance of solid media. It consists of four components as follows:

(1) The power supply component, which is made up of nitrogen bottle and chamber.

(2) The components for generating and transferring loads, consisting of the rock specimen, striking bar, input bar, and output bar.

(3) The striking velocity measuring component, consisting of spotlight, photoelectric diode, amplifier, and counter.

(4) The strain measuring component, including strain gauges and ultradynamic apparatus as well as the dynamic test and analysis equipment.

The dynamic parameter has been achieved using SHPB system with 75 mm diameter (Figure 2), which is designed by Central South University [19]. Meanwhile, the parameters of the SHPB are illustrated in Table 2.

During the SHPB experiments, high-pressure gas provided by a nitrogen bottle expands in a chamber and pushes and accelerates a striking bar which moves forward to strike the input bar at a certain speed and produces an input wave $\varepsilon_I(t)$ in the input bar. When the wave $\varepsilon_I(t)$ reaches the interface (Figure 3), two waves are produced, among which one part is reflected back along the input bar and produces the reflected wave $\varepsilon_R(t)$ and the other wave moves forward and reaches the output bar through the specimen and produces the transmission wave $\varepsilon_T(t)$. The strain pulse signals are collected via strain gauges and transformed into electric signals through ultradynamic strain equipment and then transferred into dispersed signals and stored in recorded form. All these recorded dispersed signals are analyzed all together after completing the tests.

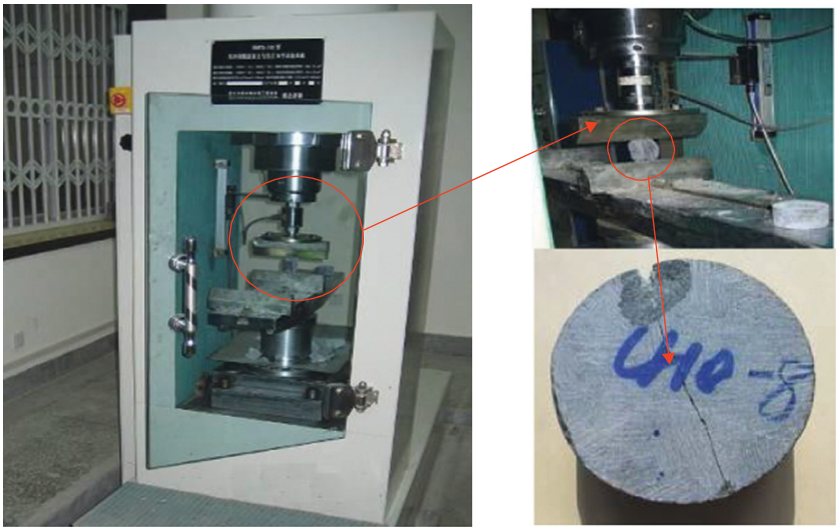

Figure 1: Rock mechanics testing system RMTS150 and specimen.

Based on the wave propagation theory and one-dimensional stress hypothesis, as well as the continuity demands of displacement, the stress and displacement of the rock specimen are calculated as follows:

$$p_1(t) = EA[\varepsilon_I(t) + \varepsilon_R(t)], \tag{5}$$

$$p_2(t) = EA\varepsilon_T(t), \tag{6}$$

$$u_1(t) = c_0 \int_0^t [\varepsilon_I(t) + \varepsilon_R(t)]\, dt, \tag{7}$$

$$u_2(t) = c_0 \int_0^t \varepsilon_T(t)\, dt, \tag{8}$$

where A, E, and c_0 refer to the sectional area, elastic modulus, and longitudinal wave velocity of the input bar or output bar, respectively.

It is assumed that the mean value of stresses from the two ends of the rock specimen can be regarded as the stress in the whole specimen, as the rock specimen is much shorter than the striking bar. Therefore, it can be expressed as follows:

$$p(t) = \frac{p_1(t) + p_2(t)}{2}. \tag{9}$$

The inertial effects are eliminated because there is no global force difference in the specimen to induce inertial forces (discussed in the following sections). Therefore, we propose a similar equation for calculating the stress intensity factor for Mode I fracture in the current specimen. The dynamic tensile strength using the Brazilian split test method is measured for obtaining rock dynamic tensile strength. And the calculation is as follows:

$$\sigma_{td} = \frac{2P_d}{\pi D t}, \tag{10}$$

where P_d is the maximum load during the impact test and D and t are the diameter and thickness of the rock specimen, respectively.

Table 1: Parameters of RMTS150.

Maximum axial direction load	Axial displacement
1500 kN (pressure)	0~150 mm
900 kN (tensile)	(±75 mm)

Figure 2: Schematics of SHPB equipment.

3.3. Testing Process. The specimens are also under air-dry condition, and the test was carried out at room temperature. Firstly, in order to verify the stability of the system, the testing system without specimen has been impacted. Secondly, the input bar has been monitored to connect the output bar closely, and then the impact waves coincide with the SHPB principle. Thirdly, the specimen with different loading speeds has been stricken using the SHPB. It should be noticed that the initial impact velocity is calculated using the static tensile strength data. Then, the strain and stress of the specimen could be obtained by the above equations, and the testing data should be checked using the dynamic force balance method. In the end, the dynamic tensile strength of the specimen tested has been calculated by means of the dynamic stress at the failure point.

The pulse shaper technique is employed to achieve dynamic force balance in the specimen during the experiment, that is, $P_1 = P_2$. In a traditional SHPB test, the incident wave with a sharp rising edge may initiate undesired damage to the

Table 2: Parameters of SHPB.

Diameter of the bar (mm)	Length of the input bar (mm)	Length of the output bar (mm)	Elastic modulus (GPa)	Longitudinal wave velocity	Poisson ratio	Pressure (MPa)	Density ($kg \cdot m^{-3}$)
75	2000	2000	250	5400	0.285	0~10	7810

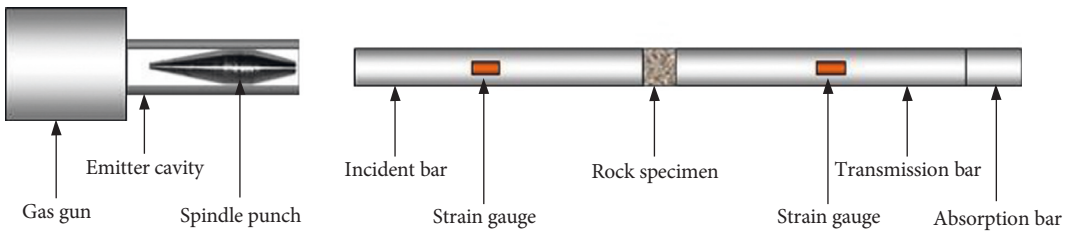

Figure 3: Schematics of SHPB setup.

sample upon impact. Consequently, the forces on both sides of the specimen are not the same, likely resulting in misinterpretation of data. We use a C11000 copper disc to shape the incident wave from the rectangular shape to a ramped wave. In addition, a rubber disc is placed in front of the copper shaper to reduce the rising slope of the incident pulse. This combined pulse shaping technique was also used by other researchers.

Figure 4 shows the forces on both ends of the specimen in a typical test. From Equation (5), the dynamic force on the one side of the specimen P_1 is proportional to the sum of the incident (In) and reflected (Re) stress waves, and the dynamic force on the other side P_2 is proportional to the transmitted (Tr) stress wave. It can be seen from Figure 4 that the dynamic forces on both sides of the specimens are almost identical during the whole dynamic loading period. The inertial effects are thus eliminated because there is no global force difference in the specimen to induce inertial force. Consequently, the inertial effects are negligible in such cases and we can then perform quasistatic analysis.

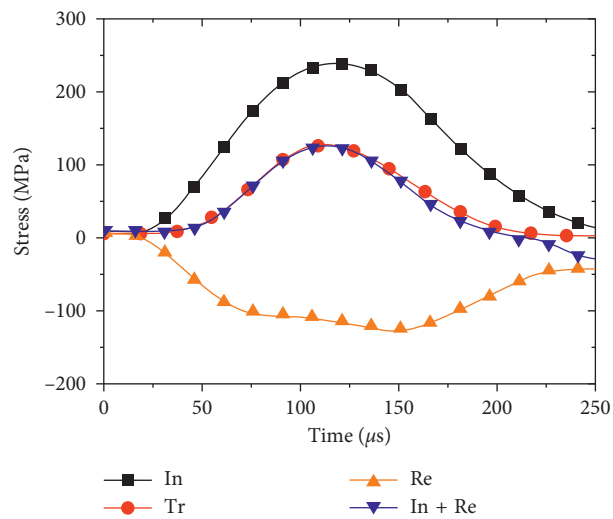

Figure 4: Dynamic force balance verified during a typical SHPB test.

4. Measurement of Dynamic Fracture Toughness

4.1. Sampling and Rock Specimen Preparation. As the purpose of this paper is to research the relationship between the dynamic fracture toughness and dynamic tensile strength of the rock, the rock specimen with the same lithology has been measured to ensure these toughness and strength tests are under the same rock properties. For the fracture toughness measurement of brittle rocks, core-based samples are preferred because they can be easily obtained from natural rock blocks. As a result, the developed standard method of fracture toughness tests on metals [20] and ceramics [21] is rarely utilized. ISRM recommended two methods with three types of core-based specimens for determining the fracture toughness of rocks: chevron bend (CB) and short rod (SR) specimens in 1988 [22] and cracked chevron notched Brazilian disk (CCNBD) specimen in 1995 [23–25]. According to "Suggested method for determining mode I fracture toughness using Cracked Chevron Notched Brazilian Disc (CCNBD) specimens" suggested by ISRM in 1995 [11], the CCNBD specimen is prepared. In order to get a more accurate toughness, the flattened CCNBD specimen has been finally manufactured [26–28]. The specimen is expressed in Figure 5, while the geometry is detailed in Table 3.

4.2. Testing Equipment and Measuring Principle. As we aimed at studying the relationship between the dynamic tensile strength and dynamic fracture toughness, the SHPB with a same size of 75 mm diameter was used in this study.

According to the fracture mechanics principle [9, 10], it could be regarded that the failure point of the dynamic fracture toughness is under the maximum load condition, as a result of the crack propagation unstably when the load decreases suddenly [9]. So, the failure point can be expressed as:

$$\frac{d\sigma}{dt} = 0. \tag{11}$$

Based on the ISRM standard for CCNBD specimen [11, 29–31], we used a similar equation for calculating the stress intensity factor for Mode I fracture in the current specimen:

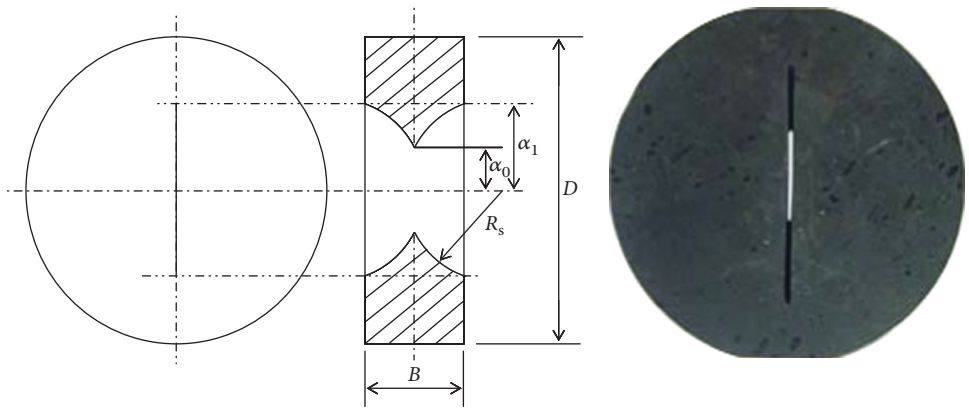

(a) (b)

Figure 5: Geometry of the CCNBD specimen recommended (a) and the flattened CCNBD specimen (b).

Table 3: Geometry of the standard CCNBD.

Descriptions	Values	Dimensionless expression
Diameter D (mm)	75	—
Thickness B (mm)	30	$\alpha_B = B/R = 0.8$
Initial chevron notched crack length a_0 (mm)	9.89	$\alpha_0 = a_0/R = 0.2637$
Final chevron notched crack length a_1 (mm)	24.37	$\alpha_1 = a_1/R = 0.65$
Saw radius R_s (mm)	26	$\alpha_s = R_s/R = 0.6933$
Dimensionless stress intensity factor	0.84	—

$$K_{Id} = \frac{P_{max}}{B\sqrt{R}} Y^*_{min}, \tag{12}$$

where K_{Id} is the dynamic fracture toughness and Y^*_{min}, a dimensionless geometry factor, is a function of the crack geometry, which can be calculated easily. And P_{max}, B, and R refer, respectively, to the maximum load during the testing process, thickness, and radius of the specimen.

Compared with Equations (11) and (12), it can be drawn that both these specimen rupture criterions are under the maximum load. It has been showed that the failure criterions are uniform. Meanwhile, it also explains that the purpose of the fracture testing is to search the maximum load corresponding to the crack propagation unsteadily.

4.3. Testing Process. The testing principle and the testing progress are also nearly the same to the dynamic tensile strength measurement. Obviously, the CCNBD specimen with different loading speeds has been stricken using the SHPB. Then, the strain and stress of the specimen could be obtained by the above equations. And the dynamic fracture toughness of the specimen tested has been calculated by means of the dynamic stress at the failure point.

5. Result and Analysis

Through the above testing and measurement, the dynamic tensile strength, dynamic fracture toughness data, and loading rate are shown in Tables 4–6, respectively. For the static tensile testing, the effective data are chosen only if the specimens are split into two parts from the central axes after the test [26, 27], or else the data should be omitted. According to the static tensile data, the initial dynamic impact velocity for the SHPB testing was determined. For the SHPB testing, the specimen usually ruptures into two or more fractions. It could be transformed from the electric signals on the strain gauge into strain data and then the

Table 4: Dynamic fracture toughness and dynamic tensile strength of 410 m.

$\dot{K}_{Id}$ (MPa·m$^{1/2}$·s^{-1})	K_{Id} (MPa·m$^{1/2}$)	σ_{td} (MPa)
111089	12.8	9.3
141265	14.7	9.8
150903	15.5	10.3
163611	15.5	10.7
165121	16.2	12.8
212652	16.8	13.9
170339	17.0	14.9
235937	17.5	16.4

Table 5: Dynamic fracture toughness and dynamic tensile strength of 510 m.

$\dot{K}_{Id}$ (MPa·m$^{1/2}$·s^{-1})	K_{Id} (MPa·m$^{1/2}$)	σ_{td} (MPa)
115945	11.7	5.7
122839	12.8	6.6
139858	14.3	6.9
159310	22.1	7.4
230667	22.1	7.9
240101	22.6	10.8
162295	23.2	10.8
207318	23.6	11.4

Table 6: Dynamic fracture toughness and dynamic tensile strength of 610 m.

$\dot{K}_{Id}$ (MPa·m$^{1/2}$·s^{-1})	K_{Id} (MPa·m$^{1/2}$)	σ_{td} (MPa)
131236	20.9	7.0
141948	21.7	7.7
160777	23.6	7.8
199820	25.9	7.9
214561	27.9	9.8
290718	30.2	14.1
338431	30.7	15.2

stress is calculated. More importantly, according to the dynamic force balance [32], the testing data should be verified whether they coincide with the basic principle of SHPB. For the satisfied data, the dynamic tensile strength and dynamic fracture toughness using Equations (10) and (12) could be obtained through the maximum load. It should be noticed that the specimens for dynamic tensile strength measurement and the specimens for dynamic fracture toughness test are both cored from the same rock. Then, the two kinds of parameters of the same specimen could be compared and analyzed together. In the meantime, the loading rate shows the ratio of the dynamic fracture toughness to the loading time, corresponding to the fracture toughness.

The calculated dynamic tensile strength, dynamic fracture toughness, and loading rate of the rock specimens from the depths 410 m, 510 m, and 610 m are illustrated in Figures 6–8, respectively.

It can be directly understood that there is an empirical relation between dynamic tensile strength and dynamic fracture toughness. Compared with Equation (2), the dynamic fracture toughness is higher than the static fracture toughness, by about one order of magnitude. And there is a relation between strength and toughness of rock. Furthermore, the dynamic fracture toughness and dynamic tensile strength increase with the loading rate. It should be noted that the dynamic tensile strength increases at faster rate than the dynamic fracture toughness.

6. Discussion

Zhang et al. [33, 34] pointed out that the fracture toughness and loading rate can be described as $K_{Id} \propto \dot{K}_I^a$, where a is a constant. And the uniaxial dynamic compressive strength of rock and the strain rate have a similar relation $\sigma_{cd} \propto \dot{\varepsilon}^a$, where a is an integer [35]. Furthermore, as we know, the uniaxial compressive strength of a given rock is usually 8–15 times greater than its uniaxial tensile strength. This means that the strength and the toughness of rock are likely to be related to each other. Zhang [15] has obtained the relation between the static fracture toughness and tensile strength, while this paper focuses on the relation between dynamic fracture toughness and dynamic tensile strength of the rock.

Why does the strength have a relation with the toughness of rock? Which one, strength or toughness, is the more essential factor to describe the rock failure? Previous studies [1–6] of compressive microfracture have suggested strongly

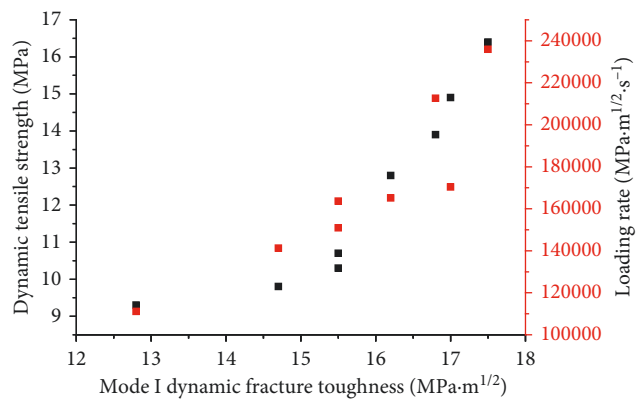

Figure 6: Relation between dynamic fracture toughness and dynamic tensile strength of 410 m.

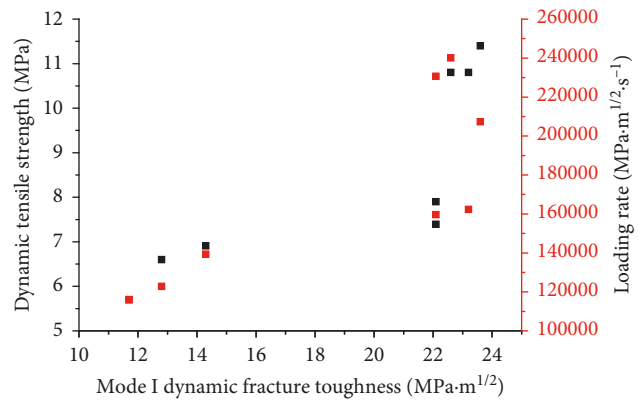

Figure 7: Relation between dynamic fracture toughness and dynamic tensile strength of 510 m.

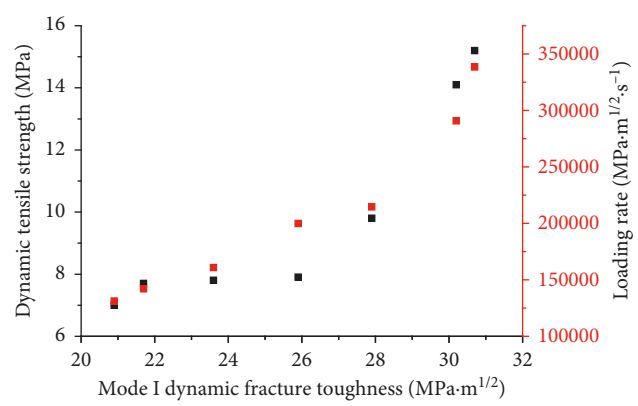

Figure 8: Relation between dynamic fracture toughness and dynamic tensile strength of 610 m.

that stress-induced microcracks in rock are caused by the tensile, rather than shearing, are axial in orientation, and are responsible for observed dilatant and hysteretic effects. It indicates that the relation between the strengths, which includes tensile strength and compressive strength of the rock, and toughness is due to a similar fracture mechanism. Rock failure in tensile, shear, and compressive strength

mainly results from microcracks induced by tensile stress. It can be considered to be one of the reasons why the tensile, shear, compressive rock strength, and static and dynamic fracture toughness are related to each other. And some authors proposed the crack propagation models [1, 2, 4, 36–39], which also confirmed the above theory. According to the mechanism, the toughness value could be calculated through the tensile strength.

Experimental observations have also shown that there are some similarities in fracture patterns occurring in the tensile strength test and fracture toughness test. For the tensile test, the entire specimen failed along the loading direction, exactly from the centre of the specimen. For the toughness test, under a lower loading rate, the specimen ruptures into two parts similar to the standard tensile test, especially from the loading direction. The specimen was shocked into several more fractions when the loading rate is higher. This phenomenon indicates that the failure of each specimen results from the extension of a single crack or the coalescence of a few microcracks in the same plane. Meanwhile, it can be observed that there are considerable clear crack branches on the fracture surface. From this point, the fracture surface formation of a specimen tested for tensile strength is similar to that for the fracture toughness.

7. Conclusions

Mode I dynamic fracture toughness and dynamic tensile strength of the rock in Beijing Datai well at different depths have been measured according to the suggested methods by ISRM and GB/T50266-2013. Two conclusions can be drawn as follows:

(1) Both the dynamic fracture toughness and dynamic tensile strength increase with loading rate.

(2) Dynamic tensile strength increases at faster rate than the dynamic fracture toughness.

Data Availability

The data used to support the findings of this study are included in Section 5 (Tables 4–6).

Conflicts of Interest

The authors declare that they have no conflicts of interest.

Acknowledgments

This work was supported by the China Scholarship Council, "State Sponsored Scholarship Program for Graduate Students," and the National Natural Science Foundation of China (Grant nos. 50674092 and 50774076). The authors are most grateful to Professor ZHAO J. for his valuable help in EPFL-LMR. The experiments were carried out at Central South University and Si Chuan University. The author would like to acknowledge Professor Li X. B. and Professor Wang Q. Z. for helping with the tests.

References

[1] H. Deng and S. Nemat-Nasser, "Dynamic damage evolution in brittle solids," *Mechanics of Materials*, vol. 14, no. 2, pp. 83–103, 1992.

[2] S. Nemat-Nasser and H. Deng, "Strain rate effect on brittle failure in compression," *Acta Metallurgica et Materialia*, vol. 42, no. 3, pp. 1013–1024, 1994.

[3] A. Golshani, Y. Okui, M. Oda, and T. Takemura, "A micromechanical model for brittle failure of rock and its relation to crack growth observed in triaxial compression tests of granite," *Mechanics of Materials*, vol. 38, no. 4, pp. 287–303, 2006.

[4] H. B. Li, J. Zhao, and T. J. Li, "Micromechanical modeling of the mechanical properties of a granite under dynamic uniaxial compressive loads," *International Journal of Rock Mechanics and Mining Sciences*, vol. 37, no. 6, pp. 923–935, 2000.

[5] A. Golshani, M. Oda, Y. Okui, T. Takemura, and E. Munkhtogoo, "Numerical simulation of the excavation damaged zone around an opening in brittle rock," *International Journal of Rock Mechanics and Mining Sciences*, vol. 44, no. 6, pp. 835–845, 2007.

[6] H. B. Li, J. Zhao, and T. J. Li, "Triaxial compression tests on a granite at different strain rates and confining pressures," *International Journal of Rock Mechanics and Mining Sciences*, vol. 36, no. 8, pp. 1057–1063, 1999.

[7] M. F. Kanninen and C. H. Popelar, *Advanced Fracture Mechanics*, Q. L. Hong, G. H. Zheng, Q. X. Zheng et al., Beijing Aviation Academy Press, Beijing, China, 1987, in Chinese.

[8] Q. Gao, *Engineering Fracture Mechanics*, Chongqing University Press, Chongqing, China, 1986, in Chinese.

[9] C. A. Tang, *Catastrophe in Rock Unstable Failure*, China Coal Industry Publishing House, Beijing, China, 1991, in Chinese.

[10] T. Y. Fan, *Dynamic Fracture Mechanics Principle and its Application*, Beijing Institute of Technology Press, Beijing, China, 2006, in Chinese.

[11] R. J. Fowell, "Suggested method for determining mode I fracture toughness using cracked chevron notched Brazilian disc (CCNBD) specimens," *International Journal of Rock Mechanics and Mining Sciences & Geomechanics Abstracts*, vol. 32, no. 1, pp. 57–64, 1995.

[12] ISRM Testing Commission, "Suggested method for determining the fracture toughness of rock," *International Journal of Rock Mechanics and Mining Sciences*, vol. 25, no. 2, pp. 71–96, 1988.

[13] Y. Yu, J. X. Zhang, and J. C. Zhang, "A modified Brazilian disk tension test," *International Journal of Rock Mechanics and Mining Sciences*, vol. 46, no. 2, pp. 421–425, 2009.

[14] B. N. Whittaker, R. N. Singh, and G. Sun, *Rock Fracture Mechanics: Principles, Design and Applications*, Elsevier, Amsterdam, Netherlands, 1992.

[15] Z. X. Zhang, "An empirical relation between mode I fracture toughness and the tensile strength of rock," *International Journal of Rock Mechanics and Mining Sciences*, vol. 39, no. 3, pp. 401–406, 2002.

[16] X. P. Xie and Z. H. Chen, *Rock Mechanics*, Science Press, Beijing, China, 2004, in Chinese.

[17] J. J. Wang, J. G. Zhu, C. F. Chiu, and H. Zhang, "Experimental study on fracture toughness and tensile strength of a clay," *Engineering Geology*, vol. 94, no. 1-2, pp. 65–75, 2007.

[18] Guojia Biaozhun-GB: GB/T 50266—2013, *Standard for Test Methods of Engineering Rock Masses*, Research Institute of Standards & Norms, Beijing, China, 2013, in Chinese.

[19] F. Q. Gong and G. F. Zhao, "Dynamic indirect tensile strength of sandstone under different loading rate," *Rock Mechanics and Rock Engineering*, vol. 47, no. 6, pp. 2271–2278, 2014.

[20] ASTM Standard E399-09, *Standard Test Method for Linear-Elastic Plane-Strain Fracture Toughness KIC of Metallic Materials*, ASTM International, West Conshohocken, PA, USA, 2009.

[21] ASTM Standard C1421-01b, *Standard Test Methods for Determination of Fracture Toughness of Advanced Ceramics at Ambient Temperature*, ASTM International, West Conshohocken, PA, USA, 2007.

[22] F. Ouchterlony, "Suggested methods for determining the fracture toughness of rock," in *The Complete ISRM Suggested Methods for Rock Characterization, Testing and Monitoring; 1974–2006*, R. Ulusay and J. A. Hudson, Eds., pp. 231–258, ISRM Turkish National Group, Ankara, Turkey, 2007.

[23] R. J. Fowell, J. A. Hudson, C. Xu, and J. F. Chen, "Suggested method for determining mode-I fracture-toughness using cracked chevron-notched Brazilian disc (CCNBD) specimens," in *The Complete ISRM Suggested Methods for Rock Characterization, Testing and Monitoring; 1974–2006*, R. Ulusay and J. A. Hudson, Eds., pp. 259–268, ISRM Turkish National Group, Ankara, Turkey, 2007.

[24] Y. X. Zhou, K. Xia, X. B. Li et al., "Suggested methods for determining the dynamic strength parameters and mode I fracture toughness of rock materials," *International Journal of Rock Mechanics and Mining Sciences*, vol. 49, pp. 105–112, 2012.

[25] Q. B. Zhang and J. Zhao, "A review of dynamic experimental techniques and mechanical behavior of rock materials," *Rock Mechanics and Rock Engineering*, vol. 47, no. 4, pp. 1411–1478, 2014.

[26] Q. Z. Wang and X. M. Jia, "Determination of elastic modulus, tensile strength and fracture toughness of brittle rocks by using flattened Brazilian disk specimen—part 1: analytical and numerical results," *Chinese Journal of Rock Mechanics and Engineering*, vol. 21, no. 9, pp. 1285–1289, 2002, in Chinese.

[27] Q. Z. Wang and L. Z. Wu, "Determination of elastic modulus, tensile strength and fracture toughness of brittle rocks by using flattened Brazilian disk specimen—part 2: experimental results," *Chinese Journal of Rock Mechanics and Engineering*, vol. 23, no. 2, pp. 199–204, 2004, in Chinese.

[28] S. M. Dong, Q. Y. Wang, and S. W. Shu, "Analysis of stress intensity factor for flattened Brazilian dick," *Conference of Study on Structural Strength*, 2008, in Chinese.

[29] F. Dai, K. Xia, and L. Z. Tang, "Rate dependence of the flexural tensile strength of Laurentian granite," *International Journal of Rock Mechanics and Mining Sciences*, vol. 47, no. 3, pp. 469–475, 2010.

[30] R. J. Fowell and C. Xu, "The use of the cracked Brazilian disc geometry for rock fracture investigation," *International Journal of Rock Mechanics and Mining Sciences & Geomechanics Abstracts*, vol. 31, no. 6, pp. 571–579, 1994.

[31] X. L. Zhao, R. J. Fowell, J. C. Roegiers, and C. Xu, "Rock fracture toughness determination by the Brazilian test, by H. Guo, N.I. Aziz, L.C. Schmidt," *Engineering Geology*, vol. 38, no. 1-2, pp. 181–184, 1994.

[32] R. Chen, K. Xia, F. Dai, F. Lu, and S. N. Luo, "Determination of dynamic fracture parameters using a semi-circular bend technique in split Hopkinson pressure bar testing," *Engineering Fracture Mechanics*, vol. 76, no. 9, pp. 1268–1276, 2009.

[33] Z. X. Zhang, S. Q. Kou, J. Yu, Y. Yu, L. G. Jiang, and P. A. Lindqvist, "Effects of loading rate on rock fracture," *International Journal of Rock Mechanics and Mining Sciences*, vol. 36, no. 5, pp. 597–611, 1999.

[34] Z. X. Zhang, S. Q. Kou, L. G. Jiang, and P. A. Lindqvist, "Effects of loading rate on rock fracture: fracture characteristics and energy partitioning," *International Journal of Rock Mechanics and Mining Sciences*, vol. 37, no. 5, pp. 745–762, 2000.

[35] X. B. Li and D. S. Gu, *Rock Impact Dynamics*, Press of Central South University of Technology, Changsha, China, 1994, in Chinese.

[36] H. Horii and S. Nemat-Nasser, "Brittle failure in compression: splitting, faulting and brittle-ductile transition," *Philosophical Transactions of the Royal Society A: Mathematical, Physical and Engineering Sciences*, vol. 319, no. 1549, pp. 337–374, 1986.

[37] H. Horii and S. Nemat-Nasser, "Elastic fields of interacting inhomogeneities," *International Journal of Solids and Structures*, vol. 21, no. 7, pp. 731–745, 1985.

[38] H. Horii and S. Nemat-Nasser, "Overall moduli of solids with micro cracks: load-induced anisotropy," *Journal of the Mechanics and Physics of Solids*, vol. 31, no. 2, pp. 155–171, 1983.

[39] S. Nemat-Nasser and H. Horii, "Rock failure in compression," *International Journal of Engineering Science*, vol. 22, no. 8–10, pp. 999–1011, 1984.